Extended Wear Testing of the 12-kW Advanced Electric Propulsion System Engineering Test Unit Hall Thruster

IEPC-2022-362

Presented at the 37th International Electric Propulsion Conference
Massachusetts Institute of Technology, Cambridge, MA USA
June 19-23, 2022

Jason D. Frieman[1], Hani Kamhawi[2], Jon Mackey[3], and Peter Y. Peterson[4]
NASA Glenn Research Center, Cleveland, OH, USA 44135

James H. Gilland[5],
Ohio Aerospace Institute, Cleveland, OH, USA 44142

Richard Hofer[6],
Jet Propulsion Laboratory, California Institute of Technology, Pasadena, CA, USA 91109

and

Derek Inaba[7], Hoang Dao[8], Nicholas A. Branch[9], and Benjamin Welander[10]
Aerojet Rocketdyne, Redmond, WA, USA 98052

This work presents a summary of the first wear test of the 12 kW Advanced Electric Propulsion System (AEPS) intended to isolate the impact of discharge current on component wear rates. Testing was led by Aerojet Rocketdyne and performed with the AEPS Engineering Test Unit 2 (ETU-2) thruster. In total, approximately 860 hours of operation were accumulated split between operating conditions of 600 V/9 kW, 600 V/11 kW, and 600 V/12 kW. Thruster performance and stability were invariant throughout the wear test for all thruster throttle conditions and shown to be equal to the values previously measured with ETU-2. Inner front pole cover erosion rates were found to be invariant to discharge current as the measurements at all three operating conditions were equal to within the empirical uncertainty. Outer front pole cover erosion rates were found to be equal for the 600 V/9 kW and 600 V/12 kW conditions with operation at 600 V/11 kW yielding elevated erosion rates. Overall, the data shows that the AEPS thruster design has a high probability of meeting lifetime and performance requirements as the design proceeds to flight production and qualification.

I. Introduction

NASA continues to evolve a human exploration approach for beyond low-Earth orbit and to do so, where practical, in a manner involving international, academic, and industry partners [1]. The center of this approach is NASA's Gateway that is envisioned to provide a maneuverable outpost in lunar orbit that extends human presence in deep

[1] Research Engineer, Electric Propulsion Systems Branch, jason.d.frieman@nasa.gov
[2] NASA AEPS Test Lead, Electric Propulsion Systems Branch, hani.kamhawi-1@nasa.gov
[3] Research Engineer, Electric Propulsion Systems Branch, jonathan.a.mackey@nasa.gov
[4] Solar Electric Propulsion Product Lead Engineer, Electric Propulsion Systems Branch, peter.y.peterson@nasa.gov
[5] Senior Scientist, Electric Propulsion Systems Branch, james.h.gilland@nasa.gov
[6] NASA AEPS Thruster Lead, Electric Propulsion Group, richard.r.hofer@jpl.nasa.gov
[7] AEPS Thruster Test Lead, derek.inaba@rocket.com
[8] Senior Electric Thruster Engineer, hoang.dao@rocket.com
[9] Electric Thruster Engineer, nicholas.branch2@rocket.com
[10] AEPS Thruster Lead, benjamin.welander@rocket.com

space and expands on NASA exploration goals. The Gateway represents the initial step in NASA's architecture for human cislunar operations, lunar surface access, and missions to Mars.

NASA announced at the May 2020 NASA Advisory Council's Human Explorations and Operations Committee a new plan that calls for launching the first two elements of Gateway as a co-manifested mission in the late 2023 timeframe [2]. Launching the Power and Propulsion Element (PPE) and the Habitation and Logistics Outpost (HALO) together reduces mission risk, utilizes the PPE high-powered Solar Electric Propulsion (SEP) system to transport both elements to lunar orbit, and reduces overall cost. NASA and Maxar Technologies have a commercial partnership to develop and demonstrate the high-powered SEP spacecraft [3, 4]. The PPE is baselined to include EP strings comprised of 12-kW Advanced Electric Propulsion System (AEPS) thrusters developed by Aerojet Rocketdyne and Busek-developed 6-kW Hall thrusters for a total beginning of life propulsion power of over 48 kW [5].

Development of the 12-kW Hall thruster was led by the NASA Glenn Research Center (GRC) and the Jet Propulsion Laboratory (JPL) and began with maturation of the Hall Effect Rocket with Magnetic Shielding (HERMeS) Technology Demonstration Units (TDUs). The technology development work transitioned to Aerojet Rocketdyne (AR) via a competitive procurement selection for the AEPS contract in May 2016. Management of the AEPS contract is being led by NASA GRC with funding from NASA's Space Technology Mission Directorate under the Technology Demonstration Missions Program. NASA continues to support the AEPS development by leveraging in-house expertise, plasma modeling capability, and world-class test facilities.

As part of the AEPS development, a series of four wear tests have been conducted to identify erosion phenomena and the accompanying failure modes as well as to validate service-life models for magnetically-shielded thrusters. The first began in 2016 and accumulated approximately 1700 hours of operation using the HERMeS TDU-1 thruster [6]. The second was performed in 2017 with the HERMeS TDU-3 thruster; this test included seven short duration (~200 hour) segments each testing a different thruster configuration or operating condition and is referred to as the TDU-3 Short Duration Wear Test (SDWT) [7]. The third wear test (named the TDU-3 Long Duration Wear Test or LDWT) began in October 2017 and was completed in October 2018 [8, 9]. It accumulated approximately 3,570 hours of total operating time split between six test segments and investigated the impacts of discharge voltage, magnetic field strength, facility pressure, and pole cover material on thruster wear rates. The LDWT also served as a pathfinder test giving NASA the opportunity to develop the experience and procedures necessary for long duration testing of high-powered Hall thrusters. The final wear test was led by AR and performed with the second engineering test unit (ETU-2) version of the 12-kW AEPS Hall thruster. Testing began in December 2019 and was completed in February 2020; this wear test accumulated approximately 730 hours of total operating time split between two wear segments [10].

To date, all TDU and ETU wear test segments have been performed over a range of discharge powers, but at a fixed discharge current (20.83 A). This test campaign expands these results by acquiring data at three additional discharge currents: 600 V/9 kW, 600 V/11 kW, and 600 V/12 kW. This test campaign was a collaborative effort led by AR and executed to their test plans and procedures with NASA support. Testing began in July 2021 and was completed in November 2021 with the overall goal to assess wear trends at these expanded throttle conditions.

II. Experimental Apparatus

A. AEPS ETU-2

All performance test data summarized in this work was collected on the AEPS ETU-2 Hall thruster designed and built by Aerojet Rocketdyne. This 12-kW thruster is derived from the NASA HERMeS TDU thrusters, and has preserved several key features of the TDU thrusters, including the magnetic shielding topology which permits a design lifetime of greater than 23,000 hours [11, 12]. The ETU thruster design also includes design updates to meet environmental and spacecraft interface requirements and improve manufacturability; these updates are intended to serve as an initial assessment of a more flight-like configuration prior to the final design phase.

B. Thruster Support Equipment

Xenon propellant was supplied to the thruster and the centrally mounted cathode using a laboratory feed system composed of electropolished stainless-steel lines metered with commercial thermal mass flow controllers. The anode line was metered using a 500-sccm controller, and the cathode line was metered using a 100-sccm controller. All controllers were calibrated using a NIST-traceable piston prover [13]. The controllers had a measured uncertainty of approximately 0.5% of the reading. This system is identical to that used in previous TDU and ETU tests [6–9].

All power to ETU-2 was provided using a power console composed of commercial laboratory power supplies. The discharge was controlled using two 15-kW (1000 V, 15 A) power supplies connected in a controller-supporter configuration. This console is equipped with a set of safety interlocks that allows the data acquisition or vacuum

facility control system to disable power and place the thruster in a safe state if a facility or thruster anomaly is detected. This setup is unchanged from previous TDU and ETU characterization and wear tests [6–9, 12, 14–16].

Following the results from the electrical configuration study performed by Peterson *et al.* [16], the ETU-2 thruster body was electrically tied to the cathode, and all conductive surfaces within approximately one meter of the thruster exit plane were insulated using dielectric sheeting [16, 17]. This was done in order to provide better control over the number of electrical coupling paths between the thruster and facility in the near-field [16, 17].

Thruster telemetry was recorded continuously at a rate of approximately 0.5 Hz using a multiplexed data acquisition system. End-to-end calibrations of the laboratory power and data acquisition systems (DAQ) were performed using a NIST-traceable digital multimeter. The resultant uncertainty was approximately 0.03% and 0.3% of the reading for measurements of voltage and current, respectively. Voltage telemetry was measured via sense lines at the interface between ETU-2 and the facility cable harness while current telemetry was measured via a set of precision shunts located in a breakout box on the air side of the thruster power feedthrough.

Three oscilloscopes were used to monitor oscillations during this work. The first two oscilloscopes were used to compute the root-mean-square (RMS) and peak-to-peak values of the discharge current, discharge voltage, cathode-to-ground voltage, keeper voltage, and thruster body voltage. These measurements were obtained over intervals of 100,000 samples at a sampling rate of 1 MS/s and recorded by the DAQ. The third oscilloscope was used to obtain waveforms of the AC components of the discharge current, discharge voltage, cathode-to-ground voltage, and keeper voltage. These waveforms consisted of 5 million points sampled at a rate of 2.5 GS/s. All oscillation data reported in this work were collected using the oscilloscopes recorded by the DAQ. For all three oscilloscopes, current measurements were acquired using 150-A AC/DC current probes while voltage measurements were acquired using high-voltage differential probes.

C. Vacuum Facility

All test segments detailed in this work were performed in VF-5 at NASA GRC. VF-5 is a cylindrical chamber measuring 4.6 m in diameter and 18.3 m in length [18]. For these tests, VF-5 was evacuated using a series of cryopumps. The cryopumps have a combined nominal pumping speed of approximately 700,000 l/s on xenon [18–20]. In order to obtain the lowest possible background pressure, the thruster was installed in the main volume of VF-5 at the same location previously used during ETU and TDU testing [6, 7]. The placement of the cryopumps relative to the thruster at this location as well as the resultant near-field background neutral distribution are described in previous work [18–20].

Facility pressure was monitored with two xenon-calibrated and one nitrogen-calibrated Bayard-Alpert style hot-cathode ionization gauges. The nitrogen-calibrated gauge (SIG 2 N_2) was located approximately 0.7 m radially outward, 0.05 m upstream, and 0.4 m below the HCT exit plane. The orifice of SIG 2 N_2 faced radially outward (i.e., away from the HCT). One xenon-calibrated gauge (SIG 3 Xe) was centered approximately 0.7 m radially outward, 0.08 m upstream, and 0.6 m below the HCT exit plane. The orifice of SIG 3 Xe faced radially outward. The second xenon-calibrated gauge (SIG 2 Xe) was mounted adjacent to and downstream of SIG 3 Xe and had a downstream-facing orifice.

All ion gauges used in this work were configured for operation with electric propulsion systems and thus had an elbow and plasma screen installed on the inlet of the gauge [21]. The housing of each gauge was also attached to facility ground via an electrical grounding strap to avoid charging effects and then insulated with dielectric sheeting. A thermocouple was installed on the exterior of each ion gauge tube; this allowed the measured pressures to be corrected for thermal effects [22]. The gauge temperatures and pressures were sampled using the same multiplexed DAQ used to record thruster telemetry [21]. Consistent with previous tests performed in VF-5, all pressures reported in this work correspond to the measurements made using SIG 3 Xe [6, 7, 12, 14–16]. The average facility operating pressure during this work was approximately 4 μTorr-Xe at a total input flow rate of approximately 22 mg/s, which matches the pressures observed during previous TDU and ETU tests [9, 10].

D. Diagnostics

1. Thrust Stand

Thrust was measured using the same null-type inverted pendulum thrust stand used in previous HERMeS TDU and AEPS ETU performance characterization and wear tests [6, 7, 12, 14–16]. The design and theory of operation of the thrust stand are detailed in several previous works [23–25].

During this test campaign, the thrust stand was operated in a null-coil configuration. In this configuration, the position of the thruster is measured by a linear variable differential transformer (LVDT) and maintained by a pair of electromagnetic actuators. The current through each actuator is controlled using a proportional-integral-differential controller that uses the LVDT signal as the input and then modulates the current through the actuators to hold the thruster stationary. The thrust is then correlated to the resultant current through one of these actuators (i.e., the null coil). The thrust stand is also equipped with a closed-loop inclination control circuit, which uses an integral controller and piezoelectric actuator to maintain the inclination measured by an electrolytic tilt sensor and thus minimize thermal drift during performance measurements.

The thrust stand was calibrated before each set of performance measurements by loading and offloading a set of known weights using an in-situ pulley system. All reported thrust measurements have been corrected for thermal drift and offsets from the desired discharge power. The resultant thrust stand uncertainty for this work is approximately ± 5 mN [26]. Propagating this uncertainty with those from the other thruster support systems yields uncertainties of approximately 0.9% and 1.7% for specific impulse and total efficiency, respectively.

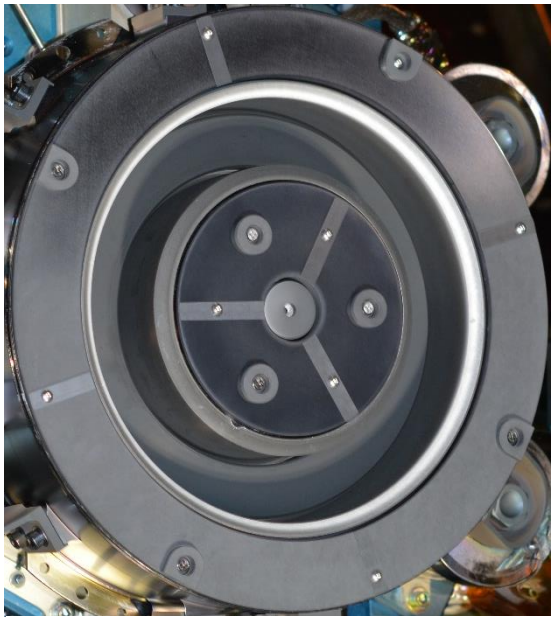


Fig. 1 Pole cover configuration used during the ETU-2 wear test segments.

2. Erosion Measurements

All erosion measurements were made with a chromatic, white-light non-contact benchtop profilometer. The employed profilometer is equipped with an optical pen oriented normal to the surface of interest with a 3-mm measuring range. All acquired profilometry data were analyzed according to the guidance established in the ISO 5436-1 measurement standard for a type A1 step (i.e., a wide groove with a flat bottom) [27]. Uncertainty was quantified using the technique detailed by Mackey et al. [28] that accounts for instrument error, surface roughness, wear due to operation at points other than the nominal wear point, and the non-flat nature of the acquired profiles. The results of this uncertainty analysis yield typical uncertainties on the order of ±2 μm for this work.

Similar to the approach taken in previous TDU and ETU wear tests, the components of greatest concern for thruster life (i.e., the pole covers) were modified in order to better characterize component erosion rates [29]. Both the graphite inner front pole cover (IFPC) and outer front pole cover (OFPC) were polished after fabrication to minimize the pre-test variation in surface roughness and provide as uniform a baseline as possible. While the entire IFPC surface was polished, only approximately one quarter of the OFPC could be polished due to limitations associated with the polishing equipment. In addition, graphite masks with a thickness of approximately 0.5 mm were installed at multiple locations on each pole cover to provide unexposed surfaces to use as a reference for post-test analysis. The corresponding pole cover configuration is shown in Fig. 1.

III. Results and Discussion

A. Test Segment Summary

Three total test segments were performed as part of this work. Segment I accumulated approximately 294 h at the 600 V/11 kW condition. Segment II was performed at the 600 V/12 kW condition and accumulated approximately 302 h of operation. The final segment was performed at the 600 V/9 kW condition and lasted approximately 267 h. At the conclusion of this test sequence, ETU-2 had accumulated approximately 2600 hours of total operation since the beginning of the development test campaign [10].

B. Performance and Oscillations

Consistent with prior wear tests of the HERMeS TDU thrusters and AEPS ETU thrusters, each test segment was book-ended by reference firing sequences in order to characterize any changes in thruster performance and stability [8, 10]. Reference firing conditions were selected to: (1) characterize non-nominal low power operations, (2) include conditions previously characterized in prior tests and (3) include operating conditions of interest for this test [30, 31]. The reference firing conditions (RFCs) used for each reference fire sequence are provided in Table 1. For all

conditions, performance was assessed at the nominal cathode flow fraction ($CFF_{nominal}$) and magnetic field strength ($B_{nominal}$).

Table 1. Extended Wear Test Reference Firing Conditions

Discharge Voltage (V)	Discharge Current (A)	Discharge Power (W)	Inclusion Rationale
300	10.00	3000	Low-power performance characterization
300	15.00	4500	
300	20.00	6000	
300	20.83	6250	Point-of-comparison to prior testing
600	20.83	12500	
600	15.00	9000	Wear test conditions of interest
600	16.67	10000	
600	18.33	11000	
600	20.00	12000	
Cathode Flow Fraction, All Conditions		1.0 $CFF_{nominal}$	
Magnetic Field Strength, All Conditions		1.0 $B_{nominal}$	

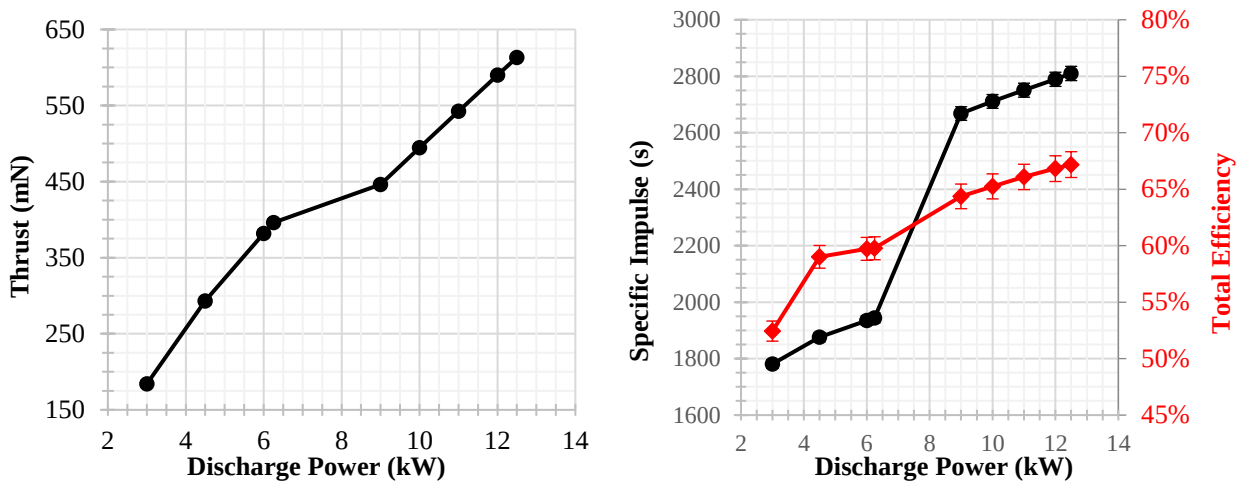
1. Thrust

The average performance of ETU-2 is presented below in Table 2, and is compared against the average of all data acquired at each set-point on ETU-2 prior to the wear test campaign. It is important to note that the performance data collected during this campaign is labeled as "Wear" throughout this work. Furthermore, it should be noted that two additional reference firing set-points (i.e., 600 V/10 kW and 600 V/11 kW) were added specifically for this test; accordingly, there exists no prior data for these conditions for comparison. These same performance results are provided visually in Fig. 2. Minimal measurements have been acquired at any condition other than 6.25 kW or 12.5 kW, thereby occluding any comparisons.

Fig. 3 and Fig. 4 show the thrust of ETU-2 at each of the RFCs from Table 1 as function of accumulated operating hours. As seen in each figure, the thrust of ETU-2 at each RFC matched the historical means to within the empirical uncertainty, at least for those RFCs previously characterized. Table 2 additionally shows that the same observation can be made for specific impulse and total efficiency. It should be noted that the definition of total efficiency has been maintained from prior works [30].

Table 2. Average Performance During the Wear Test Segments

RFC	Thrust (mN)		Specific Impulse (s)		Total Efficiency	
	Mean	Wear	Mean	Wear	Mean	Wear
300V / 3.00kW	184	184	1785	1781	52.2%	52.4%
300V / 4.50kW	294	293	1884	1876	59.6%	59.0%
300V / 6.00kW	383	382	1947	1935	60.3%	59.7%
300V / 6.25kW	395	396	1945	1944	59.6%	59.8%
600V / 9.00kW	446	446	2674	2668	64.5%	64.4%
600V / 10.00kW	-	494	-	2711	-	65.2%
600V / 11.00kW	-	543	-	2751	-	66.1%
600V / 12.00kW	591	590	2795	2789	67.0%	66.8%
600V / 12.50kW	611	613	2802	2810	66.8%	67.2%
Uncertainty	± 5 mN		± 0.9%		± 1.7%	



(a) (b)

Fig. 2 (a) Thrust and (b) specific impulse and total efficiency of the ETU-2 thruster as a function of discharge power at the Extended Wear Test RFCs.

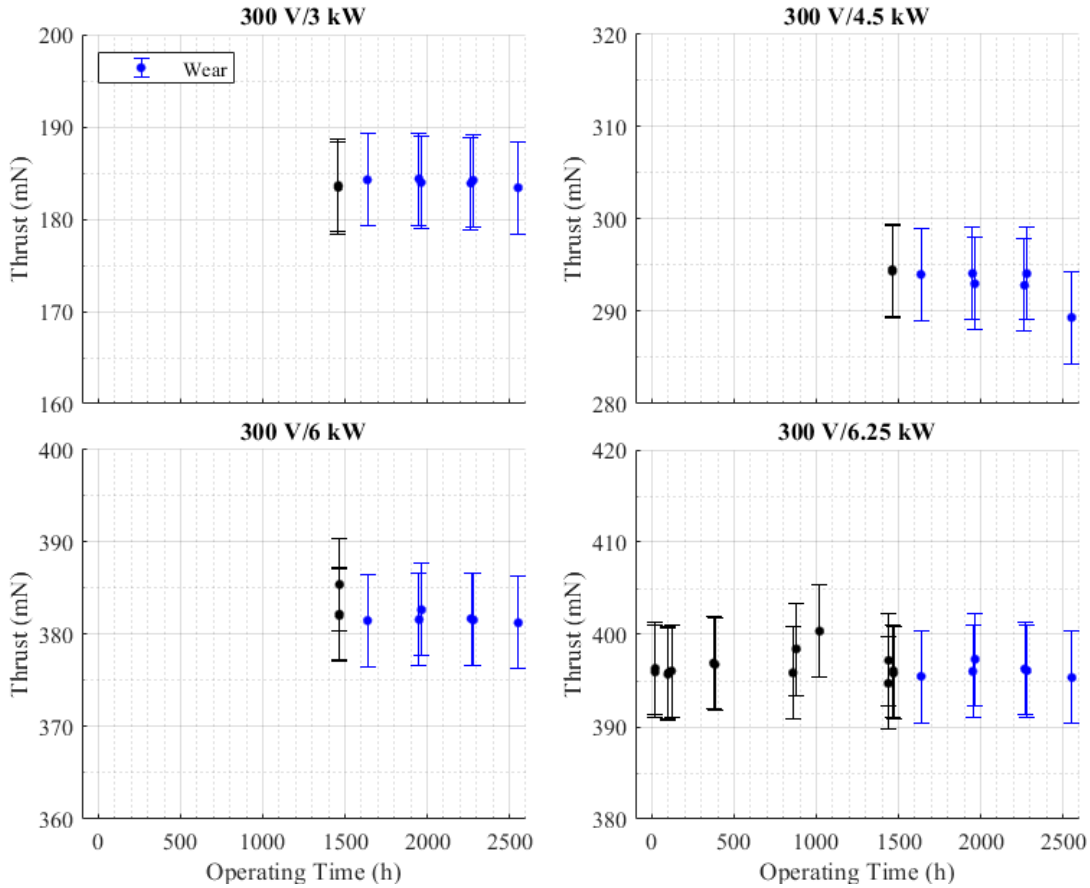


Fig. 3. Thrust of ETU-2 as a function of total operating time at the 300 V conditions.

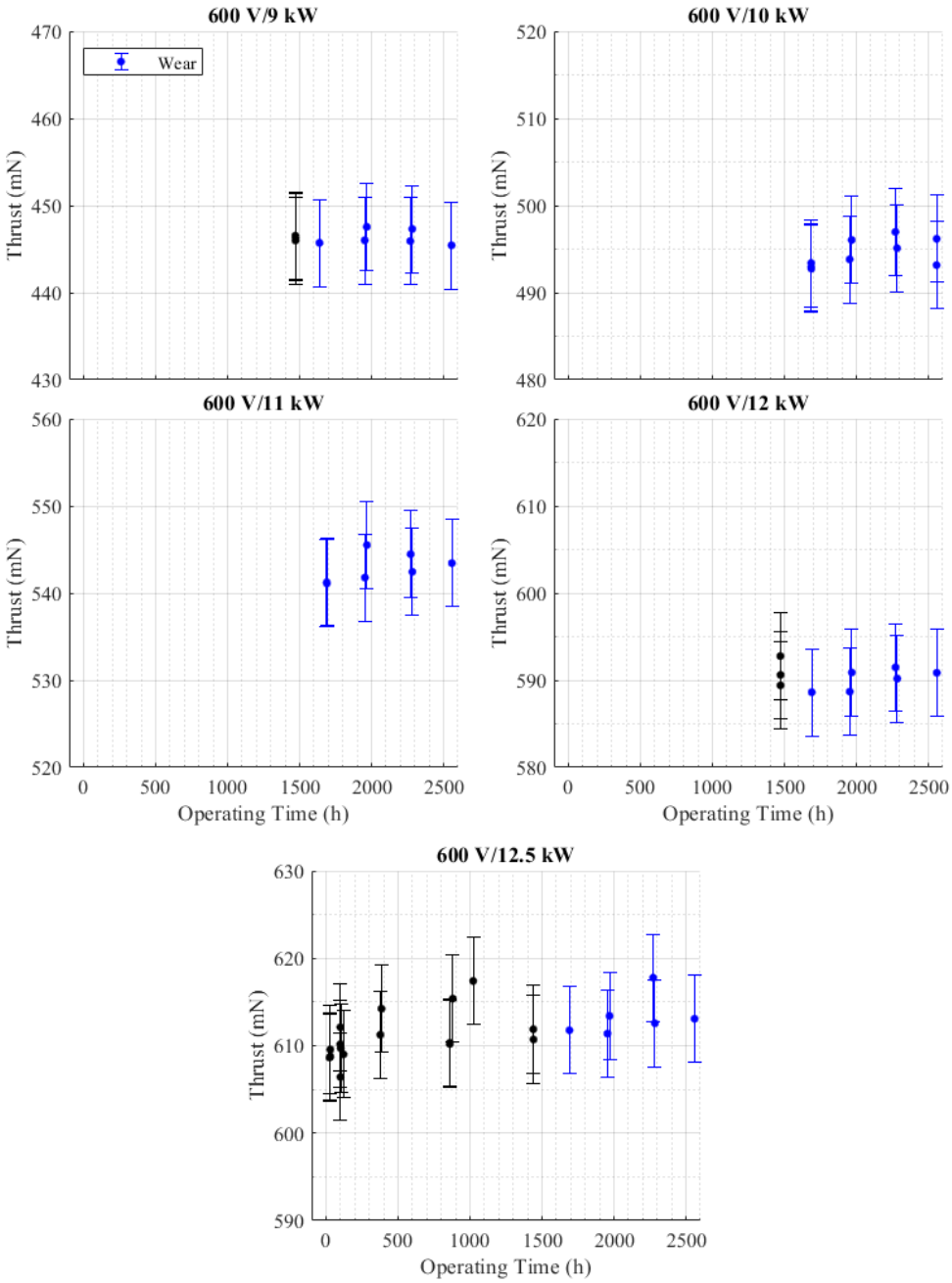


Fig. 4 Thrust of ETU-2 as a function of total operating time at the 600 V conditions.

2. Stability

Discharge ripple current was measured and tracked during each reference firing performed across this test campaign through the peak-to-peak values ($I_{D,Pk2Pk}$) and root-mean-square ($I_{D,RMS}$) values calculated from recorded discharge current waveforms. These measurements are plotted as a function of accumulated operating time and are shown in Fig. 5 and Fig. 6; peak-to-peak and root-mean-square values have been normalized by the average measured discharge current during each RFC from which the data was acquired. The ripple current data and trends are largely consistent with prior test results [10, 31]. An exception to this trend is observed at 600 V/ 12.5 kW in the bottom sub-figure of Fig. 6. A decrease in ripple current is seen between 1000 hours and 1400 hours, which corresponds to the point in ETU-2 testing where new magnetic coil currents were selected for forward testing that achieved the same overall magnetic field strength value (1.0 $B_{nominal}$). Outside of the 12.5 kW RFC, discharge ripple current has varied less than 1.35 A_{pkpk} and 0.316 A_{RMS} across all ETU-2 testing.

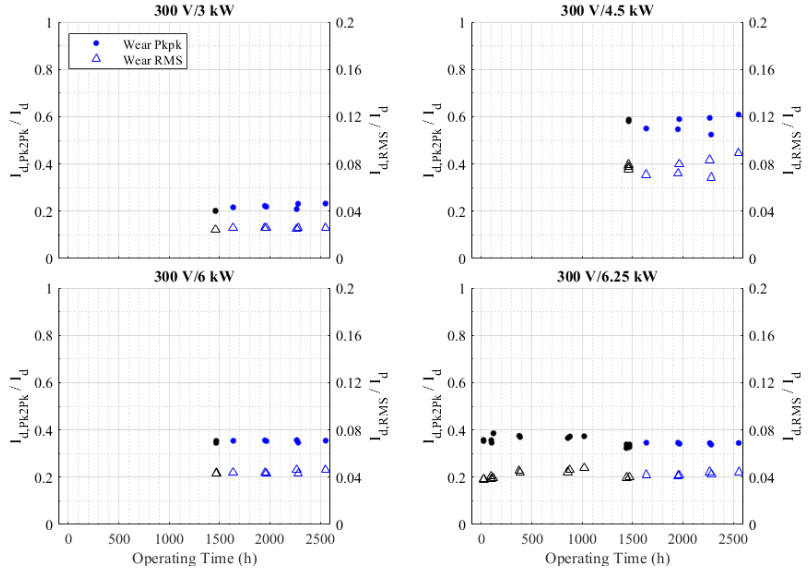


Fig. 5 Discharge ripple current of ETU-2 as a function of total operating time at the 300 V conditions.

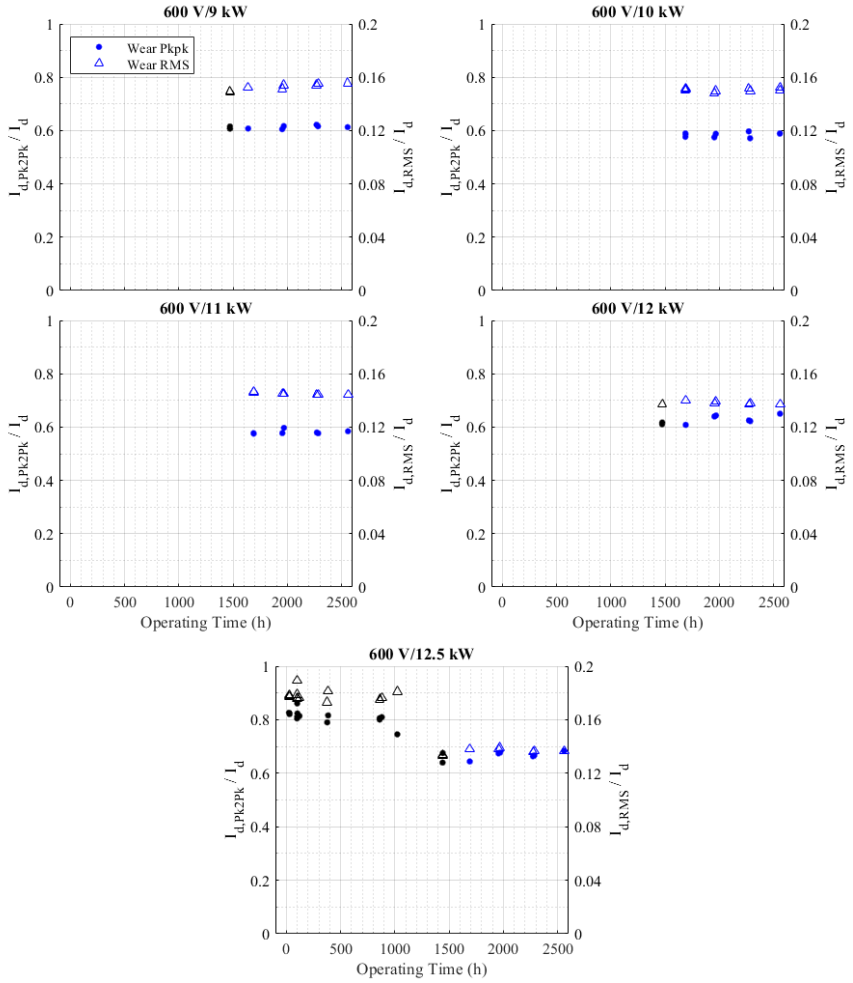


Fig. 6 Discharge ripple current of ETU-2 as a function of total operating time at the 600 V conditions.

C. Wear Results

1. *Inner Front Pole Cover*

The IFPC erosion rates measured for 600 V operation at 9 kW, 11 kW, 12 kW, and 12.5 kW are shown as a function of normalized IFPC radius in Fig. 7. In Fig. 7, a normalized radius of zero corresponds to the edge of the IFPC closest to the centrally mounted cathode whereas a radius of one corresponds to the edge of the IFPC closest to the discharge channel. Note that the truncation of the data near a normalized radius of zero is because the employed masks only covered approximately 95 percent of the IFPC, while truncation near a normalized radius of 0.5 is due to the presence of the mask fastener, which interrupted the masked region and precluded analysis in this region. In Fig. 7, the data shown for the 12.5 kW condition was acquired with TDU-3 during the work detailed in Ref. [8] while all other data were acquired with ETU-2.

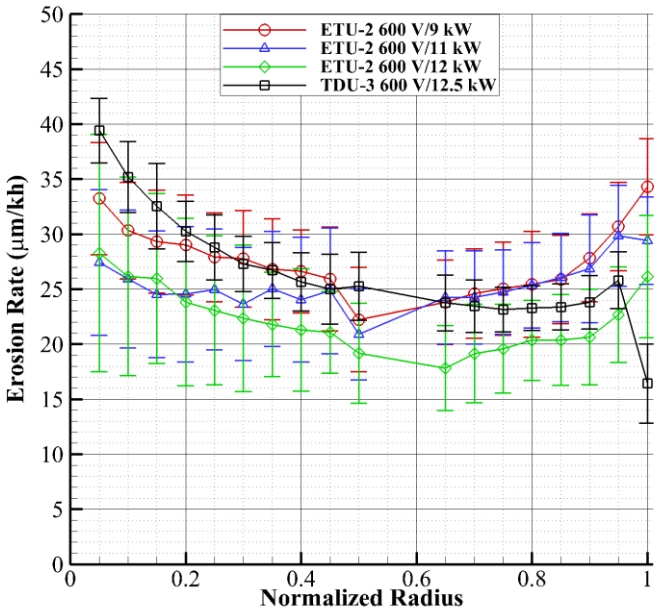
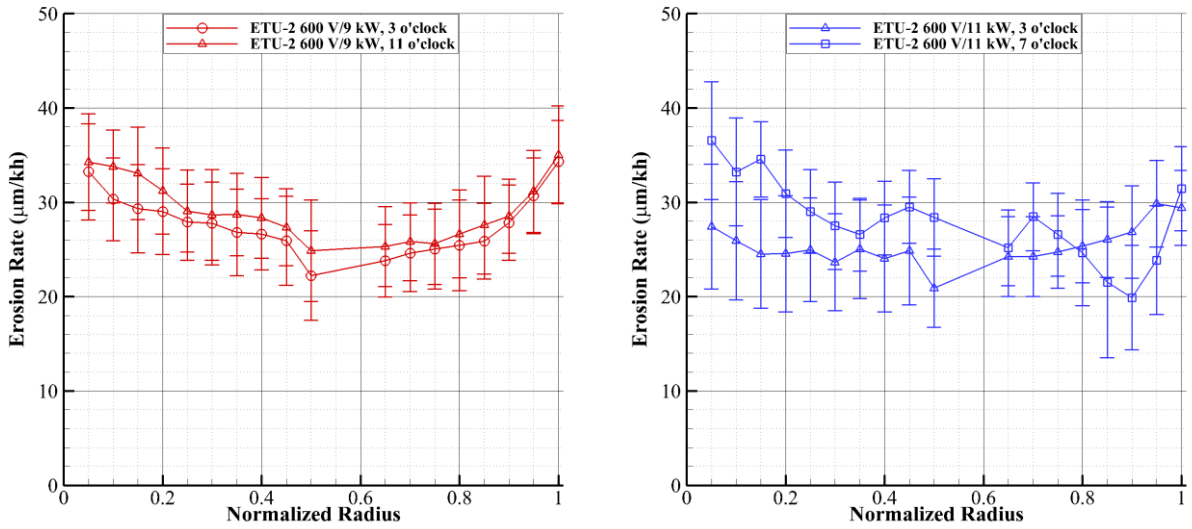


Fig. 7 IFPC erosion rates measured for 600 V operation at 9 kW, 11 kW, 12 kW, and 12.5 kW.

As shown in Fig. 7, the erosion rates measured at all four 600 V operating conditions were equal to within the empirical uncertainty. These results were confirmed by mass loss analysis, which revealed similar material loss at all four operating conditions. Further, all four IFPC erosion profiles followed nearly identical spatial profiles with minima near the center of the pole cover and maxima near the pole cover edges. This spatial profile is consistent with those observed in previous IFPC erosion measurements made with the TDU and ETU thrusters across a range of different operating conditions [29]. The 12.5 kW data contain an outlier to the overall spatial trend for the measurement at a normalized radius of one. However, the measurements in this region have a much higher measurement uncertainty due to the truncation of the unexposed reference surfaces by the edge of the IFPC. Because of this, this outlier is likely an artifact of this increased uncertainty and no strong conclusions can be drawn from it.

The IFPC erosion rates measured at two different azimuthal locations are shown for operation at 9 kW and 11 kW in Fig. 8(a) and (b), respectively. In Fig. 8, the label “xx o’clock” corresponds to the azimuthal location on the pole cover from which the data were acquired. Consistent with previous TDU and ETU measurements, the erosion rates measured at each azimuth were equal to within the empirical uncertainty for operation at both 9 kW and 11 kW, thus indicating an azimuthally symmetric wear process [29]. Unfortunately, a similar analysis could not be performed for the 12-kW condition due to poor data quality at two of the three masked locations. However, taken together, these results suggest minimal difference in IFPC wear between the new 9 kW, 11 kW, and 12 kW conditions and the extensively characterized 12.5 kW shown in previous work to have robust lifetime margins [9].



(a) **(b)**

Fig. 8 IFPC erosion rates measured at two azimuthal locations for operation at (a) 600 V/9 kW and (b) 600 V/11 kW.

2. Outer Front Pole Cover

The OFPC erosion rates measured for 600 V operation at 9 kW, 11 kW, 12 kW, and 12.5 kW are shown as a function of normalized OFPC radius in Fig. 9. In Fig. 9, a normalized radius of zero corresponds to the edge of the OFPC closest to the discharge channel whereas a normalized radius of one corresponds to the edge closest to the HCT outer diameter. Note that the truncation of the data near a normalized radius of 0 is because the employed masks do not cover the entire OFPC width, while truncation for radii greater than 0.8 is due to the presence of the mask fastener, which interrupted the masked region and precluded analysis in this region. As with the IFPC results, the data shown for the 12.5 kW condition was acquired with TDU-3 during the work detailed in Ref. [8] while all other data were acquired with ETU-2.

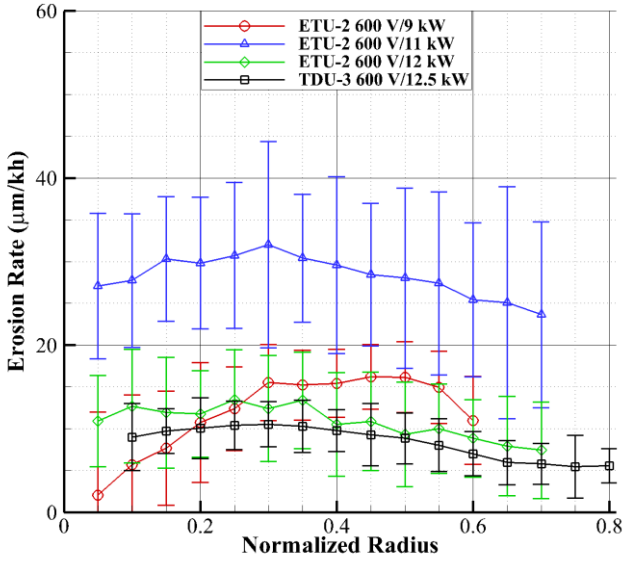
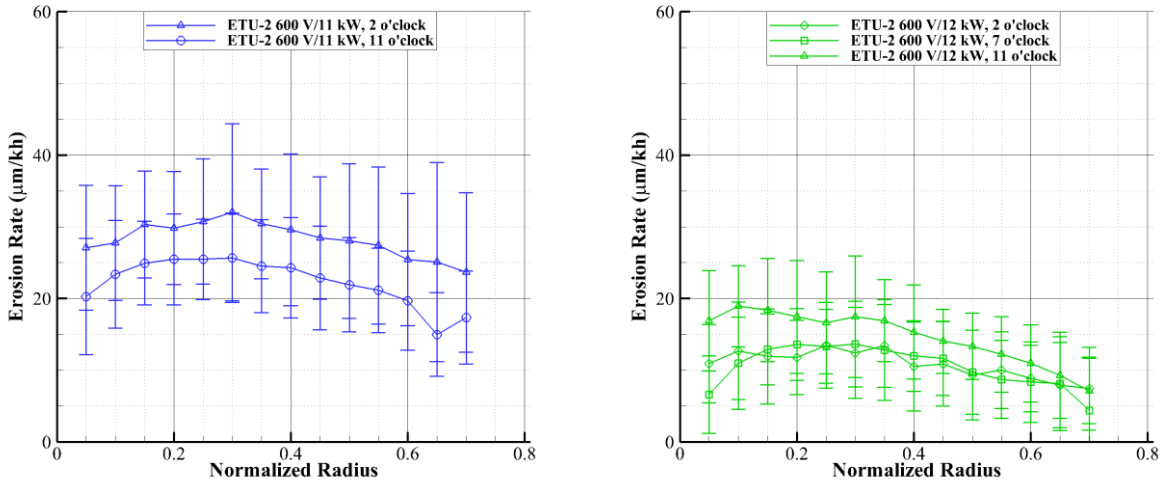


Fig. 9 OFPC erosion rates measured for 600 V operation at 9 kW, 11 kW, 12 kW, and 12.5 kW.

As was observed with the IFPC, the erosion rates measured at the 9 kW, 12 kW, and 12.5 kW conditions were equal to within the empirical uncertainty. However, the OFPC erosion rates measured at 11 kW were approximately 200% greater, on average, than those measured at the other operating conditions yielding an average erosion rate comparable in magnitude to that observed on the IFPC. This result is unique as all other tested operating conditions yielded OFPC erosion rates that were smaller than those on the IFPC [29]. However, it ultimately does not impact AEPS life estimates as the OFPC wear rates did not exceed those of the IFPC, thus leaving the latter as the most likely life-limiting component.



(a) **(b)**

Fig. 10 OFPC erosion rates measured at different azimuthal locations for operation at (a) 600 V/11 kW and (b) 600 V/12 kW.

The OFPC erosion rates measured at different azimuthal locations are shown for operation at 11 kW and 12 kW in Fig. 10(a) and (b), respectively. Consistent with previous TDU and ETU measurements, the erosion rates measured at each azimuth were equal to within the empirical uncertainty for operation at both 11 kW and 12 kW, thus indicating an azimuthally symmetric wear process [29]. It is important to note that all locations in Fig. 10 were polished prior to the test. As has previously been observed with TDU-3, no measurable erosion was detected on sections of these OFPCs that were unpolished prior to testing [29]. This precluded a symmetry analysis for the 9-kW operating condition as only one mask was in a polished region of the OFPC. Nevertheless, these results mirror those from the IFPC in suggesting minimal differences in wear between the four tested 600 V operating conditions [9].

IV. Conclusions

The results of the second wear test campaign of Aerojet Rocketdyne's AEPS ETU-2 thruster were summarized and presented herein. This test campaign accumulated approximately 900 hours split across three wear segments at the 9-kW, 11-kW, and 12-kW operating points. Performance characterizations were conducted prior to and following each wear segment to identify potential trends over life. These measurements showed that the ETU-2 performance varied by less than the measurement uncertainty throughout the test. The ETU-2 performance remained statistically equivalent to the performance of the NASA HERMeS TDU thrusters, which were documented previously [8, 9].

ETU-2 IFPC erosion rates at the 9-kW, 11-kW, and 12-kW conditions were equivalent within the measurement uncertainty. ETU-2 IFPC erosion rates were also similar to the TDU-3 erosion measurements acquired at 12.5 kW. The IFPC erosion profiles exhibited high azimuthal uniformity, consistent with results from the first ETU-2 wear test campaign [10].

ETU-2 OFPC erosion rates were equivalent to within the measurement uncertainty at 9 kW and 12 kW; the ETU-2 measurements were also similar to the TDU-3 erosion rates acquired at 12.5 kW. ETU-2 OFPC erosion rates measured at 11 kW were significantly higher than those observed at 9 kW or 12 kW, but were similar to rates observed on the IFPC. Erosion profiles on the OFPC were azimuthally symmetric, consistent with prior results [29].

The ETU-2 wear test campaign demonstrated that the rate of pole cover erosion was low enough for the AEPS thruster design to meet the 23,000-hour lifetime requirement at the new operating conditions. In combination with the thruster performance and health measurements acquired throughout wear test, the data shows that the AEPS thruster design has a high probability of meeting lifetime and performance requirements. The successful test of development hardware provides the team confidence to proceed with the Critical Design Review, flight production and qualification.

References

1 Congress, *National Aeronautics and Space Administration Transition Authorization Act of 2017*. 2017.

2 Foust, J., "NASA Refines Plans for Launching Gateway and Other Artemis Elements," *SpaceNews*, 2020.

3 Inclan, B., Anderson, G., and Russell, J., "NASA Awards Artemis Contract for Lunar Gateway Power, Propulsion," NASA, Release 19-042, 2019.

4 Herman, D. A., Gray, T., Johnson, I., Kerl, T., Lee, T., and Silva, T., "The Application of an Advanced Electric Propulsion System on the NASA Power and Propulsion Element (PPE)," *36th International Electric Propulsion Conference*, Electric Rocket Propulsion Society, IEPC Paper 2019-651, Fairview Park, OH, 2019.

5 Ticker, R., Gates, M., Manzella, D., Biaggi-Labiosa, A., and Lee, T., "The Gateway Power and Propulsion Element: Setting the Foundation for Exploration and Commerce," *2019 Propulsion and Energy Forum*, American Institute of Aeronautics and Astronautics, AIAA Paper 2019-3811, Reston, VA, 2019.

6 Williams, G., Gilland, J. H., Peterson, P. Y., Kamhawi, H., Huang, W., Swiatek, M., Joppeck, C., *et al.*, "2000-hour Wear Testing of the HERMeS Thruster," *52nd AIAA/SAE/ASEE Joint Propulsion Conference*, American Institute of Aeronautics and Astronautics, AIAA Paper 2016-5025, Reston, VA, 2016.

7 Williams, G. J., Kamhawi, H., Choi, M., Haag, T., Huang, W., Herman, D. A., Gilland, J. H., *et al.*, "Wear Trends of the HERMeS Thruster as a Function of Throttle Point," *35th International Electric Propulsion Conference*, Electric Rocket Propulsion Society, IEPC Paper 2017-207, Fairview Park, OH, 2017.

8 Frieman, J. D., Kamhawi, H., Williams, G. J., Huang, W., Herman, D. A., Peterson, P. Y., Gilland, J. H., *et al.*, "Long Duration Wear Test of the NASA HERMeS Hall Thruster," *2018 Joint Propulsion Conference*, American Institute of Aeronautics and Astronautics, AIAA Paper 2018-4645, Reston, VA, 2018.

9 Frieman, J. D., Kamhawi, H., Mackey, J., Haag, T. W., Peterson, P. Y., Herman, D. A., Gilland, J. H., *et al.*, "Completion of the Long Duration Wear Test of the NASA HERMeS Hall Thruster," *2019 Joint Propulsion Conference*, American Institute of Aeronautics and Astronautics, AIAA Paper 2019-3895, 2019.

10 Frieman, J. D., Kamhawi, H., Huang, W., Mackey, J. A., Ahern, D. M., Peterson, P. Y., Gilland, J., *et al.*, "Wear Test of the 12.5-kW Advanced Electric Propulsion System Engineering Test Unit Hall Thruster," *2020 Propulsion and Energy Forum*, American Institute of Aeronautics and Astronautics, AIAA Paper 2020-3626, Reston, VA, 2020.

11 Hofer, R. R., Polk, J. E., Sekerak, M. J., Mikellides, I. G., Kamhawi, H., Sarver-Verhey, T. R., Herman, D. A., *et al.*, "The 12.5 kW Hall Effect Rocket with Magnetic Shielding (HERMeS) for the Asteroid Redirect Robotic Mission," *52nd AIAA/SAE/ASEE Joint Propulsion Conference*, American Institute of Aeronautics and Astronautics, AIAA Paper 2016-4825, Reston, VA, 2016.

12 Kamhawi, H., Huang, W., Gilland, J., Haag, T., Mackey, J., Yim, J., Pinero, L., *et al.*, "Performance, Stability, and Plume Characterization of the HERMeS Thruster with Boron Nitride Silica Composite Discharge Channel," *35th International Electric Propulsion Conference*, Electric Rocket Propulsion Society, IEPC Paper 2017-392, Fairview Park, OH, 2017.

13 Padden, H., "Ultra Low Flow Fast Primary Gas Prover," *Measurement Science Conference*, Butler, NJ, Bios International Corporation, Butler, NJ, 2009.

14 Kamhawi, H., Huang, W., Haag, T., Yim, J., Herman, D., Peterson, P. Y., Williams, G., *et al.*, "Performance, Facility Pressure Effects, and Stability Characterization Tests of NASA's Hall Effect Rocket with Magnetic Shielding Thruster," *52nd AIAA/SAE/ASEE Joint Propulsion Conference*, American Institute of Aeronautics and Astronautics, Reston, VA, AIAA Paper 2016-4826, 2016.

15 Huang, W., Kamhawi, H., and Haag, T., "Facility Effect Characterization Test of NASA's HERMeS Hall Thruster," *52nd AIAA/SAE/ASEE Joint Propulsion Conference*, American Institute of Aeronautics and Astronautics, AIAA Paper 2016-4828, Reston, VA, 2016.

16 Peterson, P. Y., Kamhawi, H., Huang, W., Williams, G., Gilland, J. H., Yim, J., Hofer, R. R., *et al.*, "NASA's HERMeS Hall Thruster Electrical Configuration Characterization," *52nd AIAA/SAE/ASEE Joint Propulsion Conference*, American Institute of Aeronautics and Astronautics, AIAA Paper 2016-5027, Reston, VA, 2016.

17 Frieman, J. D., King, S. T., Walker, M. L. R., Khayms, V., and King, D., "Role of a Conducting Vacuum Chamber in the Hall Effect Thruster Electrical Circuit," *Journal of Propulsion and Power*, Vol. 30, No. 6, 2014, pp. 1471–1479.
18 Lobo, M. J., "Electric Propulsion Laboratory | NASA Glenn Research Center," 2017.
19 Yim, J. and Burt, J. M., "Characterization of Vacuum Facility Background Gas Through Simulation and Considerations for Electric Propulsion Ground Testing," *51st AIAA/SAE/ASEE Joint Propulsion Conference*, American Institute of Aeronautics and Astronautics, AIAA Paper 2015-3825, Reston, VA, 2015.
20 Yim, J. T., Herman, D. A., and Burt, J. M., "Modeling Analysis for NASA GRC Vacuum Facility 5 Upgrade," NASA Glenn Research Center, Cleveland, OH, NASA/TM 2013-216496, 2013.
21 Dankanich, J. W., Walker, M., Swiatek, M. W., and Yim, J. T., "Recommended Practice for Pressure Measurement and Calculation of Effective Pumping Speed in Electric Propulsion Testing," *Journal of Propulsion and Power*, Vol. 33, No. 3, 2017, pp. 668–680.
22 "Standard Practice for Ionization Gage Application to Space Simulators," ASTM International, West Conshohocken, PA, E296-70, 2015.
23 Xu, K. G. and Walker, M. L. R., "High-power, Null-type, Inverted Pendulum Thrust Stand," *Review of Scientific Instruments*, Vol. 80, No. 5, 2009, pp. 55103–55103.
24 Haag, T. W., "Thrust Stand for High-power Electric Propulsion Devices," *Review of Scientific Instruments*, Vol 62, No. 5, 1991, pp. 1186–1191.
25 Polk, J.E., Pancotti, A., Haag, T., King, S., and Walker, M., "Recommended Practices in Thrust Measurements," *33rd International Electric Propulsion Conference*, Electric Rocket Propulsion Society, IEPC Paper 2013-440, Fairview Park, OH, 2013.
26 Mackey, J., Haag, T. W., Kamhawi, H., Hall, S. J., and Peterson, P. Y., "Uncertainty in Inverted Pendulum Thrust Measurements," *54th AIAA/SAE/ASEE Joint Propulsion Conference*, American Institute of Aeronautics and Astronautics, AAA Paper 2018-4516, Reston, VA, 2018.
27 Standardization, I. O. for, "ISO 5436-1:2000 Geometrical Product Specifications (GPS) - Surface texture: Profile method; Measurement standards - Part 1: Material measures," 2003.
28 Mackey, J., Frieman, J. D., Ahern, D. M., and Gilland, J. H., "Uncertainty in Electric Propulsion Erosion Measurements," *2019 Joint Propulsion Conference*, American Institute of Aeronautics and Astronautics, AIAA Paper 2019-3896, 2019.
29 Frieman, J. D., Gilland, J. H., Kamhawi, H., Mackey, J., Williams, G. J., Hofer, R. R., and Peterson, P. Y., "Wear trends of the 12.5 kW HERMeS Hall thruster," *Journal of Applied Physics*, Vol 130, No. 14, 2021, p. 143303.
30 Frieman, J. D., Kamhawi, H., Mackey, J., Peterson, P. Y., Hofer, R. R., Inaba, D., Dao, H., *et al.*, "Extended Performance Characterization of the 12.5-kW Advanced Electric Propulsion System Engineering Test Unit Hall Thruster," *AIAA Propulsion and Energy 2021 Forum*, American Institute of Aeronautics and Astronautics, Reston, VA, AIAA Paper 2021-3431, 2021.
31 Frieman, J. D., Kamhawi, H., Huang, W., Mackey, J. A., Ahern, D. M., Peterson, P. Y., Gilland, J., *et al.*, "Characterization Test of the 12.5-kW Advanced Electric Propulsion System Engineering Test Unit Hall Thruster," *2020 Propulsion and Energy Forum*, American Institute of Aeronautics and Astronautics, AIAA Paper 2020- 3626, Reston, VA, 2020.